SUSTAINABLE WASTE MANAGEMENT & VALORISATION WITHIN THE CIRCULAR
ECONOMY ERA

Environmental impact assessment of the coal yard and ambient pollution

Marek Kucbel[1] · Helena Raclavská[1] · Karolina Slamová[2] · Michal Šafář[1] · Barbora Švédová[1] · Dagmar Juchelková[3] ·
Jana Růžičková[1]

Abstract

This study investigates the vertical distribution of pollutants emitted from coal yards using unmanned aerial vehicles (UAVs). Vertical concentration measurements of black carbon (BC) and particulate matter (PM) in a range of 1 m to 100 m above ground level (AGL) in the central coal yard showed clear spatial patterns and gradients of these pollutants. In addition, measurements were taken at specific heights (1 m, 30 m AGL, and 60 m AGL) at seven locations approximately 3 km from the yard. Thirteen measurements were carried out during the non-heating period under similar weather conditions. The measured BC concentrations decreased significantly with increasing altitude, with ground-level concentrations reaching 1.88 ± 0.61 μg/m^3 and decreasing by over 46% at 80 m AGL. Similarly, PM_{10} concentrations at 60 m AGL decreased by 21.7%, with values of 25.99 ± 9.24 μg/m^3 measured near the ground level and 16.52 ± 8.31 μg/m^3 at 60 m AGL. The maximum coal particle pollution from the coal depot ranges from 500 to 1,000 m. The study showed a significant decrease in BC concentrations with height above the coal yard surface. Concentrations of PM_{10} and PM_{10}-TSP showed a complex distribution influenced by local emissions and long-range particle transport. Meteorological factors, especially wind speed and direction, significantly influenced the pollutant dispersion. In addition, higher pollutant concentrations were measured during dry periods than after rainfall. The findings of this study contribute to a better understanding of the dispersion patterns and potential impacts of coal dust, enabling the implementation of targeted mitigation strategies and improved pollution control measures.

Keywords Coal Yard · UAV · Vertical Distribution · Air Pollution · Particulate Matter · Black Carbon

✉ Marek Kucbel
marek.kucbel@vsb.cz

1   CEET/ENET Centre, VŠB-Technical University
    of Ostrava, 17. listopadu 15/2172, 708 00 Ostrava-Poruba,
    Czech Republic

2   Institute of Foreign Languages, VŠB-Technical University
    of Ostrava, 17. listopadu 15/2172, 708 00 Ostrava-Poruba,
    Czech Republic

3   Department of Electronics, Faculty of Electrical Engineering
    and Computer Science, VŠB-Technical University
    of Ostrava, 17. listopadu 15/2172, 708 00 Ostrava-Poruba,
    Czech Republic

Introduction

Despite the increasing share of renewable energy sources in the global energy mix, coal remains an important fuel and feedstock for some industries. When coal is stored in coal yards in the open air, the effect of wind can lead to the dispersion of fine-grained particles (Wang et al. 2020), which is significant mainly at higher wind speeds (Cheng et al. 2021; Duan et al. 2023). The coal yard acts as a fugitive emission source (Woo et al. 2023), and there are economic losses (Wang et al. 2020). It is estimated that about 30% of coal particle emissions from wind erosion come from wind movement across the coal yard, 40% from the activity itself at the coal yard (coal loading and unloading), and 30% from the operation of trucks at the coal yard (Kurniawan et al. 2021).

The size of coal dust particles released from landfills ranges from < 2 μm to > 100 μm (Larson 2015). Any particles released without a size restriction are referred to as

🌻 Springer

total suspended particles (TSPs). TSPs can be divided into particles > 10 μm as well as particles < 10 μm (PM_{10}), particles < 2.5 μm ($PM_{2.5}$), and particles < 1 μm (PM_1). Coal dust particles from landfills consist of particles containing coal mass (carbon particles containing not only carbon but also H, N, S, and O) and ashes formed by minerals (mainly silicates, carbonates, and sulphides) (Ostro et al. 2023).

In the air, carbon particles are present in PM, which are formed by black carbon (BC) or elemental carbon (EC) together with organic carbon (OC). BC particles are the product of the imperfect combustion of biomass and fossil fuels from local boilers, transport, industrial sources, and power plants (Wyche et al. 2020). Black carbon has adverse impacts not only on human health, particularly the respiratory (Nducol et al. 2021) and cardiovascular systems (Rovira et al. 2022), but also on the environment, where it reduces visibility and absorbs sunlight (Nducol et al. 2021). In urban European air, BC contributes to 5–15% of mass concentrations of PM (Cavalli et al. 2016).

PM_{10} emissions in the coal yard operations are influenced by dust reduction measures and meteorological conditions but also by the intensity and technology used in coal loading/unloading (Kim et al. 2020), wind erosion from coal deposits and coal particle re-suspension (Rojano et al. 2016). The spatial distribution of the particles is influenced by the coal heap height, grain size composition, and petrographic type of coal (Kurniawan et al. 2021), moisture in the surface layer of coal (Techarat and Tontiwachwuthikul 2020), as well as operations on unpaved surfaces and maintenance of local roads (Rojano et al. 2016). Results of emission factors (EF) determined according to the US EPA methodology showed that PM_{10} from coal yards represents about 4.71E-05 g/m^2s. Of this, 27% is due to emissions generated by wind erosion and 73% is related to activities such as coal loading and unloading and operations on unpaved surfaces around coal deposits (Rojano et al. 2016). Jha and Muller (2017) found that a 10% increase in coal reserves (number of deliveries) results in a 0.06% (0.12%) increase in average levels of $PM_{2.5}$ concentrations within a radius of about 40 km in the wind direction from the place of origin. This increase in $PM_{2.5}$ concentrations brings a risk to the local population in the direction of the airflow from the coal deposit and to areas and periods with lower precipitation (Jha and Muller 2017). Pollution caused by coal dust has a considerable impact on adjacent housing, residents' health, productivity, and quality of life (Jin et al. 2022). The dust dispersion from open coal yards has become a significant issue that needs to be addressed with appropriate attention (Duan et al. 2023).

Horizontal and vertical air pollutant concentration profiles are significant for understanding air pollutant behaviour regarding air quality prediction. Different methods are used for vertical measurement of pollutant profiles, and the use of UAVs (Unmanned Air Vehicles), commonly known as drones (Lee et al. 2022), is growing in popularity. The availability of UAVs has improved significantly due to rapid technological progress (Poormorteza et al. 2022), low prices, access to hazardous and inaccessible areas and a very user-friendly interface. These features make UAVs an attractive tool for scientific research in various areas (Giordan et al. 2020; Poormorteza et al. 2022). There are obstacles to the adoption and standardisation of measurements using drones, such as limited operating hours and the payload capacity of drones. In addition, the rotary-wing propellers of a drone generate a so-called downwash, which can negatively affect the quality of the measured data. However, chemical monitoring systems based on UAVs are an excellent alternative or complement to traditional ground techniques (Burgués and Marco 2020).

The UAV platform is stable, safe and capable of providing high-resolution three-dimensional measurements of air pollutants and meteorological parameters (Samad et al. 2022). Concentrations of BC up to 100 m from the ground usually decrease with height (Chilinski et al. 2016). Vertical profiles from 0 to 120 m above ground level (AGL) confirmed higher concentrations of air pollutants at the surface due to the proximity of emission sources. PM concentrations decreased with height, and $PM_{2.5}$ decreased by 0.2 μg/m^3 per 10 m. BC concentrations had a variety of vertical profiles with a total decrease of 0.1 μg/m^3 per 10 m (Liu et al. 2020; Samad et al. 2022). In addition to local emissions, meteorological parameters play an important role in the vertical spread of PM and BC, particularly relative air humidity, wind direction and speed, atmospheric stability, and regional transport of air pollutants (Liu et al. 2020; Samad et al. 2022). Temperature inversion also influences the increase in ground BC concentrations (Chiliński et al. 2018). The vertical distribution of PM varies significantly depending on the time of year and the time of day, but in most cases, the PM concentration decreases with increasing height from the surface (Liu et al. 2021b; Dubey et al. 2022b, a). In addition to meteorological factors, the PM concentration is significantly influenced by the height of the boundary layer (Jin et al. 2020).

Most previous studies have focused on research and monitoring of PM in the ground layer. These studies have provided information on the horizontal distribution of particulate matter (PM) and other pollutants on the surface. However, in order to understand the spread of air pollution better, it is essential to understand the vertical distribution of concentrations of pollutants. Most of the previous research on the environmental impact of landfills has dealt with the issue of particle distribution in terms of size: $PM_{2.5}$, PM_{10}, and TSP (Blackwood and Wachter 1978; Davis and Boegly 1978; Mueller et al. 2015a, b; Kim et al. 2020; Woo et al. 2023). The studies are mainly focused on the properties of air pollutants and the variables influencing them in horizontal ground measurements. There is a lack of information

on the vertical dispersion of air pollutants from coal yards, which can significantly influence the overall range of pollution from a fugitive source.

This study uses modern approaches to assess the vertical distribution of dust particles from coal yards and their impact on the environment in urban agglomerations. The results presented in this paper provide completely new and unique insights into the vertical dispersion of coal particles and enable the determination of the emission impact of coal yards on the environment. This important information from coal yards was not available in the previous literature and has not been analysed using this method before.

Materials and methods

The UAV DJI Matrix 600 Pro (DJI Technology Co., Shenzhen, China) with dimensions of 1,668 mm (rotor diameter) $\times$ 727 mm (height), weighing 9.5 kg and carrying capacity of up to 6 kg was used for vertical measurements. During the measurements, the drone ascended vertically from the ground to 60 m at a constant rate of 2 m/s. The measurements occurred at ground level (1 m), 30 m, and 60 m above ground level (AGL) for 180 s. The UAV was operated in accordance with the legislative requirements for safe civilian use of drones in each category and subcategory (as open, specific, or certified) under the EU Easy Access Rules for Unmanned Aircraft Systems (Regulations (EU) 2019/947 and 2019/945) (European Commission 2019a, b).

Method of determination of the concentration of dust particles and black carbon

The elevation profile was obtained by measuring dust particles with the Fidas® Frog (Palas, Karlsruhe, Germany) and the BC aethalometer MicroAeth/MA2000 Aethlab, San Francisco, USA). In order to minimise the effect of air turbulence caused by rotor action, the Tygon® Teflon sampling hose with a length of 1,500 mm is used for the measurements on both instruments. The measured data was stored in an internal memory from which it was downloaded after the measurements were completed. The data was measured at the climb of the UAV.

The Fidas® Frog optical counter was used to measure the concentrations of the dust particles. The device is able to measure the concentrations of PM_1, $PM_{2.5}$, PM_4, PM_{10}, and TSP, as well as the number of particles at the same time. The measurement range for the mass concentration ranges from 0 to 100 mg/m^3; for the numerical concentrations, it is 0 to 20×10^9 particles/m^3. This device works with a volume flow rate of 1.4 L/min (Palas 2023). From the point of view of monitoring and assessing the impact of pollution from coal yards, PM_{10} and PM_{10}-TSP have proved to be the key coarse-grained dust particles. For this reason, we focused on the detailed characteristics of these above-mentioned dust particles, which provide detailed information on their composition, origin, and distribution in the air. From the point of view of assessing the composition of $\sum$TSP, the dust particles were divided into grain size classes: $PM_{<1}$, $PM_{1-2.5}$, $PM_{2.5-10}$, and PM_{10}-TSP.

The principle of determining the concentration of black carbon (BC) is to measure the attenuation of a beam of light passing through a quartz fibre filter, on which aerosol particles are continuously captured. MicroAeth/MA200 was used to measure BC; it is suitable for compact UV-IR BC monitoring with five wavelengths (375, 470, 528, 625, and 880 nm) with an automatic filter tape displacement system. It is also equipped with sensors for recording GPS, temperature, and relative humidity. For quantitative and qualitative determination of BC, concentrations obtained from a near-infrared channel (880 nm) of a micro-aethalometer were used (AethLabs 2018). The selected wavelength of 880 nm corresponds to the quantitative BC value, while the influence of other light-absorbing aerosols is negligible (Hansen 2005). The detection limit of MA200 is 30 ng/m^3 at a time resolution of 1 s, with a flow rate of 150 mL/min (AethLabs 2018). The data recording interval for MA200 was set to 10 s. This interval was chosen deliberately due to the absence of negative values in the 10-s time interval following optimised noise reduction. The averaging processing indicates that a satisfactory smoothing effect is achieved for black carbon concentrations (Liu et al. 2021a).

Meteorological parameters were measured by a professional digital weather station at a ground level located in the town of Karviná, operated by the Health Institute based in Ostrava.

Software

Statistical analysis for descriptive statistics, correlation analysis, and the one-way analysis of variance (ANOVA) was performed using the statistical software OriginPro 8.5 and Origin Pro2019. For correlation analysis, the Spearman correlation coefficient at the level of significance $\alpha = 0.05$ was used. The hierarchical cluster analysis (HCA) was performed using the statistical software Statgraphics Plus 5.1 (Statistical Graphics Corp.).

For constructing the model of isolines of two monitored variables at three elevation levels, the program Surfer, version 2021 (Golden Software, Inc.) was used. Input data were subjected to exploratory data analysis. The Kolmogorov–Smirnov test and Shapiro–Wilk test at the level of significance $\alpha = 0.05$ were used to test the normality of data sets. The model was constructed using kriging (linear model of variogram, without drift). The most suitable model was selected based on the results of cross-validation.

HYSPLIT model

HYSPLIT backward trajectories were used to study air mass transport, long-range transport, dispersion, and source of air pollutants. The backward trajectories were modelled in the HYSPLIT (Hybrid Single Particle Lagrangian Integrated Trajectory Model) program provided by the NOAA Air Resource Laboratory (Stein et al. 2015; Rolph et al. 2017). It is a Lagrangian model that primarily works with the pre-vailing values for wind direction and strength at the time of measurement. The Global Assimilation System (GDAS) model, with a $1° \times 1°$ resolution, was used to obtain the meteorological data. The output of the model is a map of the path of the air mass towards the location under investigation. The starting point for measuring the backward trajectories was the geographical centre of the study area (centre of the coal yard: latitude: 49°49′26.7" N, longitude: 18°29′02.1" E). The return trajectories were modelled for single measurements in 2022 for 24 h at 100 m above ground level (AGL).

Site description

The studied area (Fig. 1) is the coal yard PKP Cargo Karviná Barbora (Karviná-Doly, Moravian-Silesian Region, Czech Republic) is situated in the area of the logistics and distribution centre Upravárenský závod Karviná (ÚZK) located in the area of the former Barbora Mine. The facility was built in 2004–2005. The area is situated in a locality strongly influenced by mining activities between the towns of Karviná and Havířov in the Ostrava-Karviná coal basin. In the immediate vicinity of the studied locality, there is the heating plant Teplárna Karviná (Veolia Energie ČR), administrative buildings and production sites, which served as the background of the mine. In the vicinity, there is a situated Ridera Bohemia facility dealing with recycling and sales of inert materials. Other potential dust sources include the heating plant Teplárna ČSA (Veolia Energie ČR). Total emissions of solid pollutants (TZL) weighing 6,694 tonnes (Czech Hydrometeorological Institute 2023a) were reported from the heating plant Teplárna ČSA for the year 2021 and 7,803 tonnes (Czech Hydrometeorological Institute 2023b) from the heating plant Teplárna Karviná. The area of interest also includes the company Depos Horní Suchá, which operates the waste dump (used for the category of other wastes). Finally, there are the Remíza Pond, the Pilňok Pond, and other areas owned by the state enterprise DIAMO without any further specification of their use. This location thus provides an ideal area for monitoring the distribution of coal particles in the vicinity of the coal yard. The nearest residential development is located about 600 m from the site.
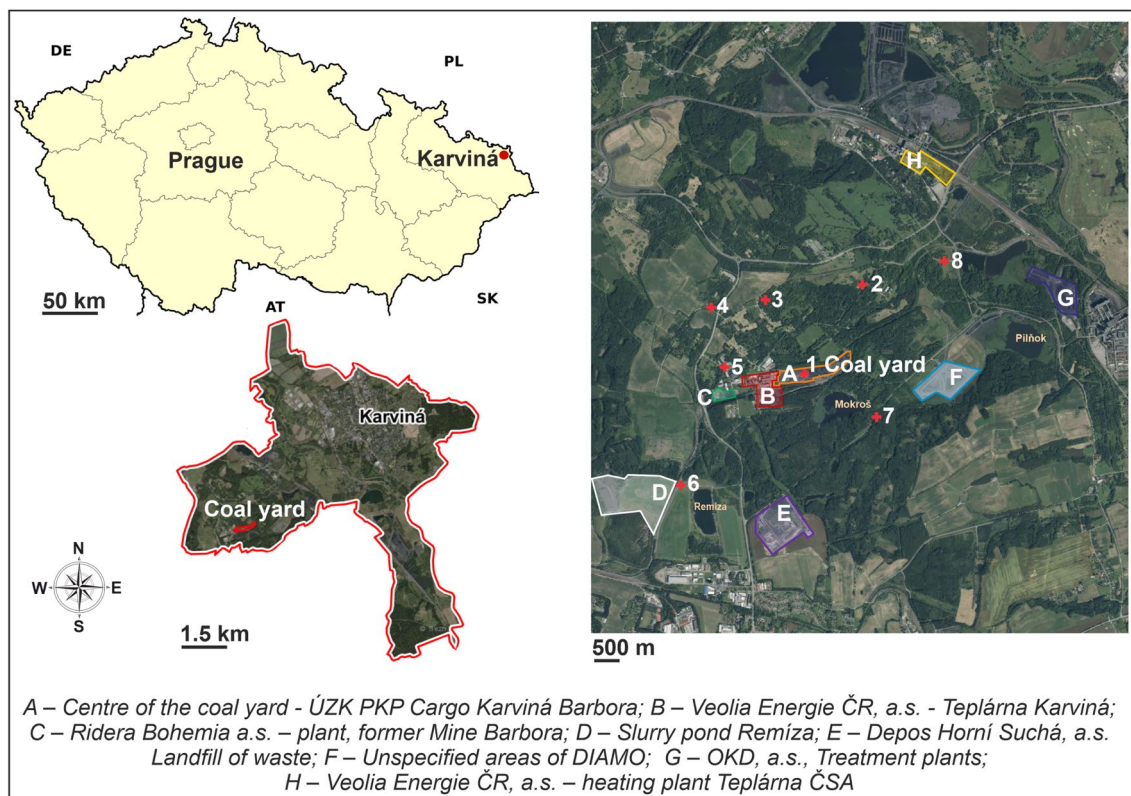

A – Centre of the coal yard - ÚZK PKP Cargo Karviná Barbora; B – Veolia Energie ČR, a.s. - Teplárna Karviná;
C – Ridera Bohemia a.s. – plant, former Mine Barbora; D – Slurry pond Remíza; E – Depos Horní Suchá, a.s.
Landfill of waste; F – Unspecified areas of DIAMO; G – OKD, a.s., Treatment plants;
H – Veolia Energie ČR, a.s. – heating plant Teplárna ČSA

Fig. 1 The position of the measured locations in the topographical map

The deposition of contaminants at the locality is influenced by significant sources of pollution in the agglomeration, in winter by the long-distance transmission of air pollution from Poland, and locally by local sources (home heating in winter).

The Barbora coal yard covers an area of about 0.85 km^2 with a maximum capacity of 200,000 tonnes of fossil fuels (bituminous coal + coke). At the time of the measurement, about 41% of the capacity of the coal yard was used. The coal yard contains bituminous coal from the Upper Silesian Coal Basin (Poland and Northern Moravia – Karviná) and the USA (Appalachian Coal Basin, West Virginia, Beckley Mine with different grain sizes from < 10 mm to 100 mm). The coal yard, where fossil fuels – coke and coal are stored, uses measures to reduce dust particles, such as spraying the site with tanker lorries and, in extreme conditions, the use

of a fogging machine. Dust control measures include limited lorry speeds, reduced drop heights for material handling and fogging equipment, etc.

The vertical distribution of black carbon and PM around the coal yard was monitored during 2022 (Table 1 and Fig. 1). Individual measurements (n = 13) were carried out in the morning (from 9:00 to 12:00) between May and October 2022. The measurements were carried out altogether at eight sites: four times in July, three times in June and August, and once in May, September, and October. The periods were chosen to reflect similar meteorological conditions and suitable conditions for UAV flight. The individual measurement days in 2022 are visualised in Fig. 2. Based on the results of the 2021 measurements, the following altitudes were selected to monitor the vertical distribution of particles at eight sites: ground level, 30 m, and 60 m AGL. In 2021, the

Table 1 Measuring sites for the study area with GPS coordinates

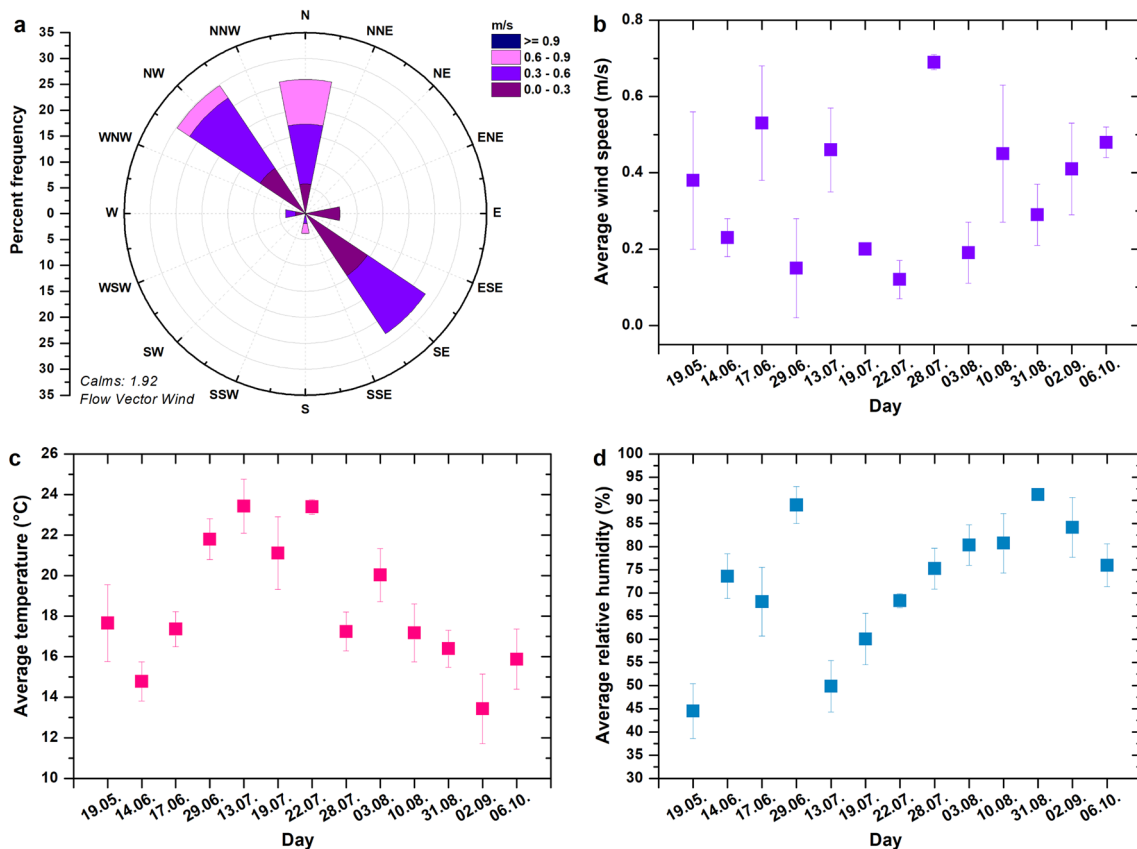| Site number	1	2	3	4	5	6	7	8
GPS_Lat	49.824085	49.832466	49.830391	49.829307	49.824724	49.813482	49.82087	49.835078
GPS_Lon	18.483913	18.491069	18.478053	18.470752	18.472962	18.468511	18.494456	18.501574

Fig. 2 Wind rose for the coal yard area during the measurements carried out in 2022 (n = 13) (**a**); basic meteorological parameters recorded during the measurements in 2022 (n = 13) – average wind speed (**b**); average temperature (**c**); average relative humidity (**d**)

vertical distribution of black carbon, PM_{10} and PM_{10}-TSP was monitored at altitudes 1 (ground level), 10, 20, 30, 40, 60, 80, and 100 m above the surface of the coal heap (AGL). The measurements of the vertical distribution of coal and dust particles were carried out only at the centre of the coal yard area (site 1) from February to November 2021 with a monthly frequency (10 measurements). The measurements were carried out under favourable dispersion conditions, allowing the use of UAV.

At the site of ÚZK PKP Cargo, Barbora, all-year-round (365 days) conditions of very mild flow prevail with wind speeds of 0–5 m/s with prevailing SW, SE, and E wind directions. During the measurements made in 2022 (13 measurements), NW, SE, and N wind direction prevailed (Fig. 2). The average air temperature at which measurements were made was 18.43 ± 3.34 °C, wind speed 0.35 ± 0.19 m/s, relative air humidity $72.41 \pm 14.47\%$, and air pressure 1024.3 hPa.

Results and discussion

The measurement results obtained from the sensors and mobile analysers attached to the UAV depend fundamentally on the position of its location on the drone, the type of UAV used, the characteristics of the load used (e.g., weight) and the target use (Burgués and Marco 2020). The most suitable location is the isolation of the sensor technique for detecting air contaminants in the lower airflow from the rotor propellers, e.g., by extending the sampling tube (Falabella et al. 2018). Accurate data was obtained during the altitude measurement with the UAV during the ascent, but during the descent, the concentrations were about 50% overestimated (Hedworth et al. 2022). In order to ensure accuracy and efficiency, it is recommended during the vertical measurement to collect only the data at the UAV exit and, at the same time, to place the suction tube under the centre of the UAV to avoid stability problems.

Vertical distribution of air pollutants from 1 to 100 m AGL over the centre of the coal heap and selection of suitable height for further measurements

For vertical measurements carried out in 2021 (Fig. 3) only at site 1 (coal yard ‑ CY), the centre of the coal heap (10 measurements) at ground level (1 m AGL) to 100 m AGL, statistically significant polynomial dependencies were found between height and concentration of BC ($r=0.93$, $\alpha=0.05$), PM_{10} ($r=0.93$, $\alpha=0.05$), and PM_{10}-TSP ($r=0.83$, $\alpha=0.05$). For the determination of the differences in concentrations of air pollutants (BC, PM_{10} and PM_{10}-TSP) between individual heights (ground level to 100 m AGL) and in individual months, they were verified using the one-way ANOVA method. Differences between the measured values were confirmed only on the days of the occurrence of maximum and minimum concentrations. The maximum concentration was measured at the time of operation of intensive heavy equipment at the coal yard.

The TSP was dominated by coarse-grained particles of the grain size class PM_{10}-TSP, which, on average, accounted for $56.37 \pm 11.34\%$ of the $\sum$TSP at all monitored heights of 1–100 m AGL. In contrast, minimal concentrations of air pollutants were demonstrated during calm airflow. In this case, the $\sum$TSP had a high proportion of fine-grained PM

Fig. 3 (**a**) Demonstration of UAV DJI flight over a coal heap body; (**b**) Average concentrations of BC particles above the centre of the coal heap body
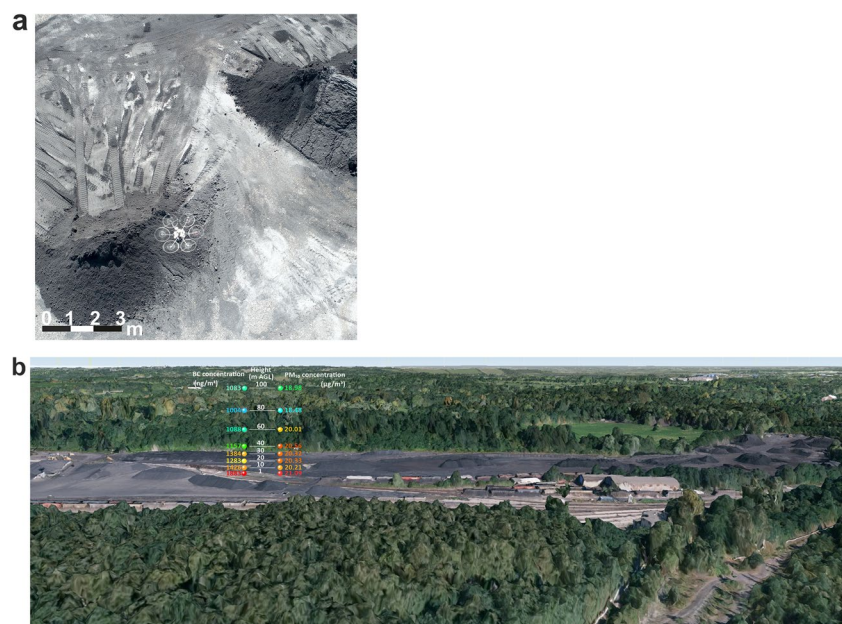
particles < 1 μm, which was $80.62 \pm 4.58\%$ at the monitored height of 1–100 m AGL; it corresponds to the origin of the particles from long-distance transport.

The average concentration (10 measurements) of BC particles decreases with increasing height from the coal surface (Fig. 4). The highest average concentration of BC particles was found for ground level $1{,}883 \pm 613$ ng/m^3. In contrast, the lowest concentration ($1{,}004 \pm 720$ ng/m^3) was measured at 80 m AGL. The difference between the highest and lowest BC concentration was 879 ng/m^3; the decrease in BC particle concentration was thus more than 46% at 80 m AGL.

The highest average concentration of PM$_{10}$ (21.09 ± 10.38 μg/m^3) was found at ground level, with concentrations decreasing slightly as the height from the surface increased. The lowest average concentration of PM$_{10}$ was found at 80 m AGL at 16.52 ± 8.31 μg/m^3, representing a 21.7% decrease in PM$_{10}$ concentration compared to ground level, with the average concentration of PM$_{10}$ increasing again at 100 m AGL to 19.80 ± 8.81 μg/m^3.

In the case of PM$_{10}$-TSP, the highest average concentrations for the ground level were also found (8.88 ± 10.85 μg/m^3). Up to 60 m above the surface of the coal heap, the TSP concentration decreases by approximately 34% from the ground level. From a height of 80 m, the PM$_{10}$-TSP

concentration increases again (Fig. 4). The distribution of PM$_{10}$ and PM$_{10}$-TSP particles depending on height has a polynomial character, characterised by a decrease in particle concentration from the ground level to 60 m AGL, followed by an increase caused by another source predominantly of inorganic particles or by long-distance transport. These results correspond to the findings reported by Samad et al. (2022). Hakala et al. (2022) found that anthropogenic air contaminants mostly occur at ground level and are trapped within the boundary layer, particularly in periods shorter than one week.

For the area of interest, it was found that the amount of PM$_{10}$ and PM$_{10}$-TSP decreases with height, which is in line with the results found for PM$_{10}$, PM$_{2.5}$, and PM$_1$ (Deng et al. 2015). Monitoring of the distribution of PM$_{10}$ by balloon over fugitive emission sources (tailings, landfills) in the Ostrava region revealed that for most fugitive sources, such as tailings and landfills, the increased concentration of PM$_{10}$ occurs at the height of 30 to 40 m above the source (Štrbová et al. 2017). The increase in concentration may be influenced by the presence of an inversion layer, which is formed at an altitude above 350–365 m above sea level, which corresponds to an altitude of 123–138 m AGL (Štrbová et al. 2017). Monitoring of PM$_{10}$ concentration by
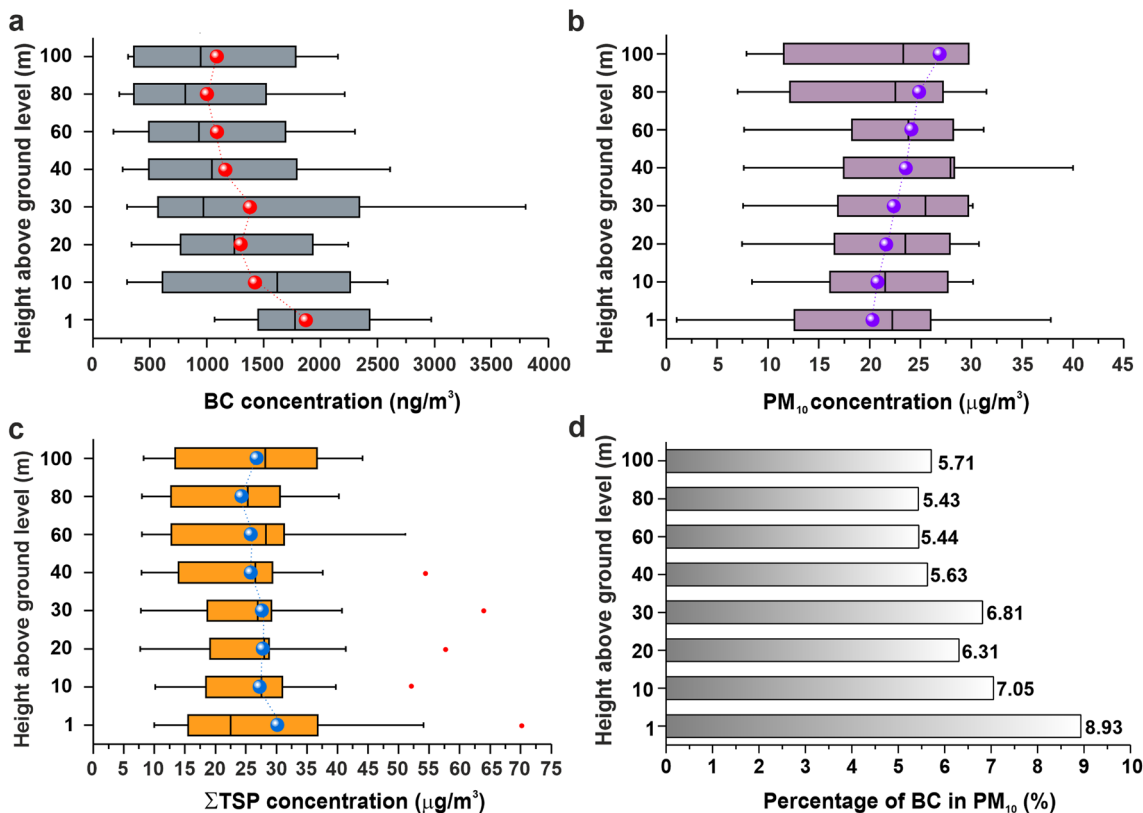

Fig. 4 (**a**) Box plot for vertical distribution of average black carbon concentrations; (**b**) PM$_{10}$; (**c**) $\sum$TSP; (**d**) percentage of BC in PM$_{10}$ measurements at the centre of the body of the coal heap at altitudes of 1 to 100 m AGL between February and November 2021

UAV in Krakow (Poland) showed three vertical zones of potential air pollution (Sekuła et al. 2021). The first zone (up to approximately 60 m above sea level) has the worst pollution conditions, which occur during periods of low wind speed when air pollution is potentially highest and lasts for a long time. The second zone, between 60 and 100 m above sea level, is a transitional zone with high levels of PM_{10}, but a significant decrease is observed with height. The third zone (above 100 to 120 m above sea level) has significantly better air quality than the first zone, which may be due to increased wind speed, wind direction changes or advection of clean air masses (Sekuła et al. 2021).

The results of the UAV measurements in 2021 showed that the coal yard affects the occurrence of BC particles up to a height of up to 30 m and most significantly at ground level, with BC concentrations in PM_{10} representing around 9% (Fig. 4). For this reason, the heights of 1 m (ground level), 30 m, and 60 m AGL were selected for the 2022 measurements.

From individual measurements, the correlation between the concentration of BC and PM_{10} was calculated for individual heights. A significant correlation between BC and PM_{10} was demonstrated only for the height of 10 m AGL, where the BC content of PM_{10} is highest.

Detailed analysis and impact on the vertical distribution of dust particles over the coal yard and surrounding area

Geochemical background and anomalies

The geochemical background and geochemical anomaly threshold values for BC, as well as PM_{10} and PM_{10}-TSP dust particles, were calculated for the 2022 assessment of the environmental load in the coal yard area (Table 2). The geochemical background value represents the arithmetic mean of all measured values for the whole monitored area. The geochemical anomaly threshold was determined as the geochemical background value increased by twice the standard deviation value according to ISO 19258:2018 "Soil quality – Guidance on the determination of background values". The statistical significance of the differences in the concentration of air pollutants in the coal yard and its wider surroundings was monitored by one-way ANOVA. The significance of the differences in concentration of BC, $PM_{<1}$, $PM_{1-2.5}$, $PM_{2.5-10}$, and PM_{10}-TSP at 1, 30 and 60 m AGL between sites was assessed. The differences in concentrations of air pollutants at 1, 30, and 60 m AGL between sites on one sampling day and on all sampling days were also evaluated. The results of one-way ANOVA did not show a difference between site No. 1 (coal yard) and seven other nearby sites for BC concentrations or PM.

Differences in geochemical background values for both BC and PM concentrations at different heights are negligible (Table 2).

Average concentrations of air pollutants depending on height for individual locations

A comparison of the values of BC, PM_{10} and PM_{10}-TSP (Fig. 5) for the body of the coal heap (CY) and for the sites in the vicinity (sites number 2–8) shows that the average BC concentrations above the coal yard at ground level ($1,330 \pm 322.8$ ng/m^3) are 17.6% higher than at the sites in the vicinity ($1,096 \pm 322.2$ ng/m^3). A similar trend can be seen at the height of 60 m AGL, where BC concentrations above the coal yard ($1,255 \pm 360.1$ ng/m^3) were 16.1% higher than at the other sites ($1,053 \pm 314.5$ ng/m^3). Only at the height of 30 m AGL were the average BC concentrations comparable for the coal yard ($1,121 \pm 351.5$ ng/m^3) and for the sites in the vicinity ($1,123 \pm 323.5$ ng/m^3). BC concentrations at this height in the area under review reach a comparable value (corresponding to the background value for 30 m AGL) and cannot be linked to coal yard activities.

The average PM_{10} concentrations for the coal yard at ground level (25.99 ± 9.24 μg/m^3) were about 3.15 μg/m^3 (12.1%) higher than for other sites in the surrounding area (22.84 ± 9.20 μg/m^3). The difference between the average

Table 2 Values of geochemical background and anomaly threshold

| AGL	BC (ng/m^3)			PM_{10} (μg/m^3)			PM_{10}-TSP (μg/m^3)		
	GL	30 m	60 m	GL	30 m	60 m	GL	30 m	60 m
Geochemical background	1125.47	1123.19	1078.94	23.24	23.42	22.85	16.36	15.02	15.37
Standard deviation	329.72	322.03	323.37	9.14	9.79	9.64	11.19	10.02	10.73
Geochemical anomaly threshold	1784.91	1767.25	1725.68	41.51	42.99	42.13	38.74	35.06	36.84
Minimal value	348.17	405.58	355.42	8.67	7.78	6.58	0.01	0.01	0.01
Median	1134.67	1127.17	1091.63	20.60	21.16	20.57	18.94	16.01	16.21
Maximum value	1900.08	1897.83	1702.33	38.97	43.31	40.15	43.46	40.60	41.11
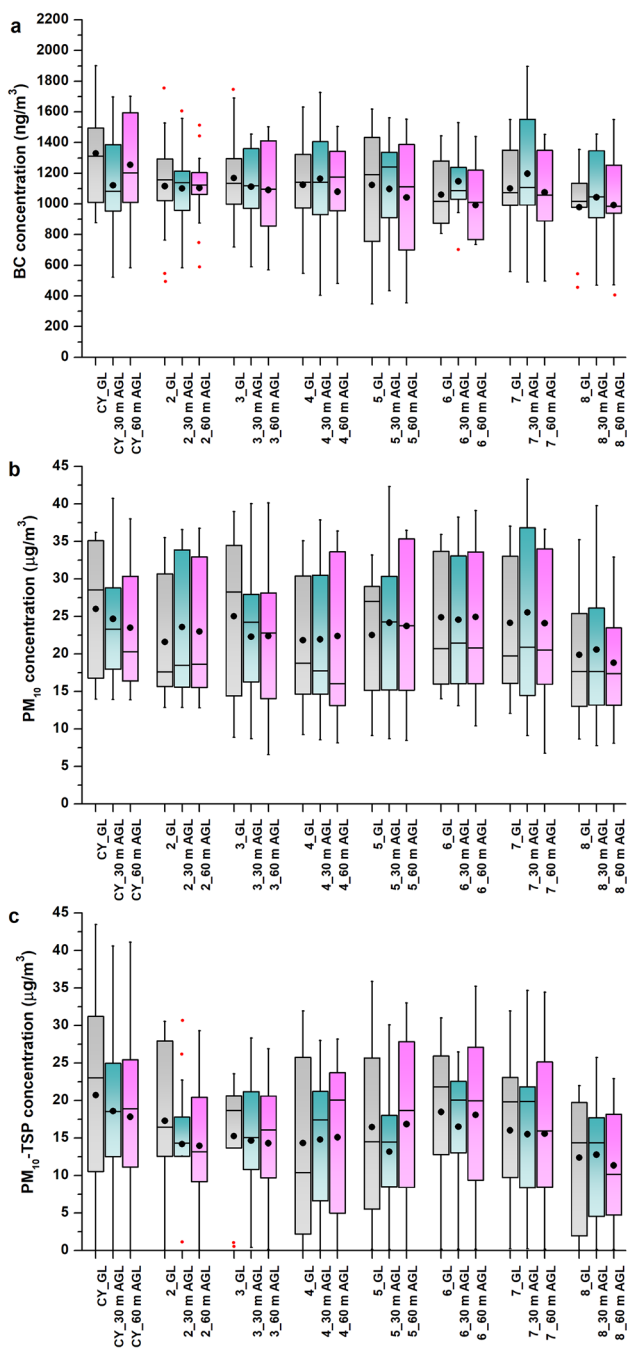
Fig. 5 (**a**) Box plot for concentrations of BC; (**b**) PM$_{10}$; (**c**) and PM$_{10}$-TSP at ground level, 30 m AGL, 60 m AGL above the body of the coal yard and for sites in the surrounding area

PM$_{10}$ concentrations for the coal yard and other sites was less pronounced for a height of 30 m AGL (1.44 μg/m^3 – 5.9%) and for a height of 60 m AGL (0.74 μg/m^3 – 3.14%). The most significant difference was observed for coarse-grained particles of the PM$_{10}$-TSP grain size class. The average PM$_{10}$-TSP concentrations at ground level were about 24% (i.e., 4.99 μg/m^3) higher for the coal yard than for sites in the

surrounding area. As the height from the surface increases, this difference decreases to 22% (4.07 μg/m^3) for 30 m AGL and 15.6% (2.79 μg/m^3) for 60 m AGL (Table 3). More coarse-grained PM$_{10}$-TSP dust particles contribute to the increased dustiness of the coal heap, which, due to weight, quickly sediment at the site of their formation and are not transported over greater distances.

The average PM$_{10}$ concentrations found at the centre of the PKP Cargo coal yard are slightly higher than reported by Mueller et al. (2015a) but are consistent with results published in other studies (Table 4). Measurements of PM$_{10}$ at four sites near an open-pit coal mine in northern Colombia showed that average concentrations were found to be twice as high during the dry season as during the wet and transition period from 14.2 ± 4.8 μg/m^3 to 55.5 ± 21.2 μg/m^3 (Arregocés et al. 2022).

The modelling of dust particles used information on the distribution of PM$_{10}$ concentrations, which are mainly influenced by the operation of coal yards. Directive 2008/50/EC of the European Parliament and of the Council of 21 May 2008 on ambient air quality and cleaner air for Europe, as amended, sets the value of the daily air pollution limit for PM$_{10}$ at 50 μg/m^3 with a maximum permitted number of exceedances of 35 times per year and the annual average value must not exceed 40 μg/m^3. None of the sites surveyed exceeded the daily air pollution limit for PM$_{10}$ in a single case. The average PM$_{10}$ concentrations at all sites were around 23 μg/m^3 at ground level. This value represents about half of the daily air pollution limit allowed. At the same time, this value complies with the recommended average 24-h PM$_{10}$ concentration of 45 μg/m^3 recommended by the global air quality guidelines of the World Health Organisation (WHO 2021).

Distribution of air pollutants in the vertical direction and cluster analysis

The average values for each site (Table 3 and Fig. 6) show no significant dispersion of dust and BC particles from the coal yard. The extent of pollution from the coal yard can be estimated to be between 500 and 1,000 m maximum. Average concentrations of PM$_{10}$ were higher than the centre of the coal yard at 30 m AGL for site No. 7 only (by about 0.86 μg/m^3) and at 60 m AGL for sites No. 5, 6, and 7. Only average concentrations of PM$_{10}$-TSP were higher at the centre of the coal yard for all measured heights, except for 60 m AGL for site No. 6. The coal yard does not significantly increase the air pollution load in the surrounding area. Higher air pollution loads were recorded at sites Nos. 5 and 6 (Fig. 6). BC particles remain at the source site, in particular at the centre of the coal yard at ground level and at 60 m AGL. The horizontal dispersion of BC is limited to a maximum of 0.5 km. Conversely,

Table 3 Basic statistical parameters of concentrations of PM10, PM10-TSP, and BC particles at individual locations

		GL				30 m AGL				60 m AGL			
		Mean	SD	Min	Max	Mean	SD	Min	Max	Mean	SD	Min	Max
CY_BC	ng/m^3	1330.10	322.79	877.09	1900.10	1121.25	351.46	521.94	1697.31	1255.26	360.05	584.18	1702.32
CY_PM$_{10}$	µg/m^3	25.99	9.24	13.97	36.22	24.68	9.48	13.93	40.74	23.49	8.98	13.89	38.00
CY_PM$_{10}$-TSP	µg/m^3	20.73	14.32	0.01	43.46	18.58	13.06	0.01	40.60	17.81	13.52	0.01	41.11
2_BC	ng/m^3	1115.29	357.83	494.75	1756.44	1101.01	308.03	583.44	1601.66	1104.43	255.38	589.08	1515.60
2_PM$_{10}$	µg/m^3	21.60	8.40	12.88	35.52	23.58	9.19	12.86	36.59	22.99	9.03	12.83	36.75
2_PM$_{10}$-TSP	µg/m^3	17.29	11.36	0.02	30.55	14.20	9.54	0.01	30.58	13.95	9.66	0.01	29.30
3_BC	ng/m^3	1168.83	338.86	720.15	1748.11	1112.87	282.68	589.66	1456.00	1090.78	308.61	570.74	1502.58
3_PM$_{10}$	µg/m^3	25.03	11.10	8.87	38.97	22.28	8.56	8.70	40.04	22.40	10.28	6.58	40.15
3_PM$_{10}$-TSP	µg/m^3	15.26	8.63	0.43	23.56	14.63	9.52	0.43	28.35	14.30	9.33	0.15	26.90
4_BC	ng/m^3	1124.67	335.59	547.34	1632.91	**1164.78***	371.43	405.58	1727.08	1079.88	341.65	480.73	1504.59
4_PM$_{10}$	µg/m^3	21.83	9.47	9.25	35.07	21.95	10.04	8.58	37.87	22.38	11.21	8.14	36.38
4_PM$_{10}$-TSP	µg/m^3	14.33	12.23	0.01	31.93	14.77	10.05	0.06	27.98	15.09	10.89	0.05	28.21
5_BC	ng/m^3	1124.09	427.50	348.19	1618.73	1097.53	373.91	434.41	1560.97	1042.30	413.43	355.41	1552.23
5_PM$_{10}$	µg/m^3	22.53	8.45	9.11	33.19	24.16	10.58	8.71	42.33	**23.71***	10.38	8.47	36.47
5_PM$_{10}$-TSP	µg/m^3	16.45	12.15	0.10	35.87	13.17	9.30	0.11	30.09	16.84	11.51	0.04	33.00
6_BC	ng/m^3	1060.11	216.23	807.00	1443.72	**1147.75***	229.25	705.81	1529.41	992.02	237.84	734.48	1440.61
6_PM$_{10}$	µg/m^3	24.88	8.89	14.01	35.93	24.55	9.53	13.10	38.26	**24.93***	9.80	10.42	39.11
6_PM$_{10}$-TSP	µg/m^3	18.46	11.38	0.16	31.02	16.52	9.53	0.16	26.48	**18.09***	11.62	0.16	35.24
7_BC	ng/m^3	1101.75	285.48	558.41	1549.27	**1196.82***	364.84	491.90	1897.83	1075.03	280.00	497.75	1452.57
7_PM$_{10}$	µg/m^3	24.15	9.44	12.09	37.02	**25.54***	12.22	9.11	43.31	**24.08***	10.27	6.76	36.63
7_PM$_{10}$-TSP	µg/m^3	16.02	10.61	0.24	31.96	15.51	11.17	0.21	34.68	15.56	11.58	0.19	34.47
8_BC	ng/m^3	979.01	294.07	455.64	1375.89	1043.57	334.28	470.82	1454.52	991.81	363.89	409.16	1551.12
8_PM$_{10}$	µg/m^3	19.88	8.67	8.67	35.24	20.59	10.03	7.78	39.79	18.81	8.31	8.10	32.92
8_PM$_{10}$-TSP	µg/m^3	12.37	8.77	0.05	21.99	12.77	8.96	0.11	25.73	11.33	8.19	0.11	22.92

Explanation: * – concentration of the parameter higher than the average value above the centre of the coal yard

Table 4 Comparison of PM$_{10}$ concentrations with literature

Area	Site	Season	PM$_{10}$ Mean	Max	Ref
Coal yard—Gallatin Power Plant (USA)	Downwind site 2	June-November 2012	14.3	134	[a]
	Downwind site 3	June-November 2012	11.5	146	
	Downwind site 2	June-November 2012 Without activity*	19.7		[b]
	Downwind site 3	June-November 2012 Without activity*	21.1		
	Downwind site 2	June-November 2012 With activity*	60.7		
	Downwind site 3	June-November 2012 With activity*	59.9		
Coal yard—UNI Power Plant Iowa (USA)	South-Windward side	July–October 2008	34.49	77.83	[c]
	North-Leeward side	July–October 2008	26.94	48.64	
Coal yard—PKP Cargo,Barbora,Karviná (CR)	Centre-Ground level	May–October 2022	25.99	36.22	This study
	Centre-30 m AGL	May–October 2022	24.68	40.74	
	Centre-60 m AGL	May–October 2022	23.49	38.00	

Explanations: *Average upwind and downwind PM$_{10}$ concentrations adjusted to the concentration of C_{xs}* for hours without and with human activity in the coal yard (adjusted concentration C_{xs}* provided a consistent measure of coal yard impact on downwind particulate levels across all hours); [a] – Mueller et al. (2015a); [b] – Mueller et al. (2015b); [c] – Wittenburg (2018)
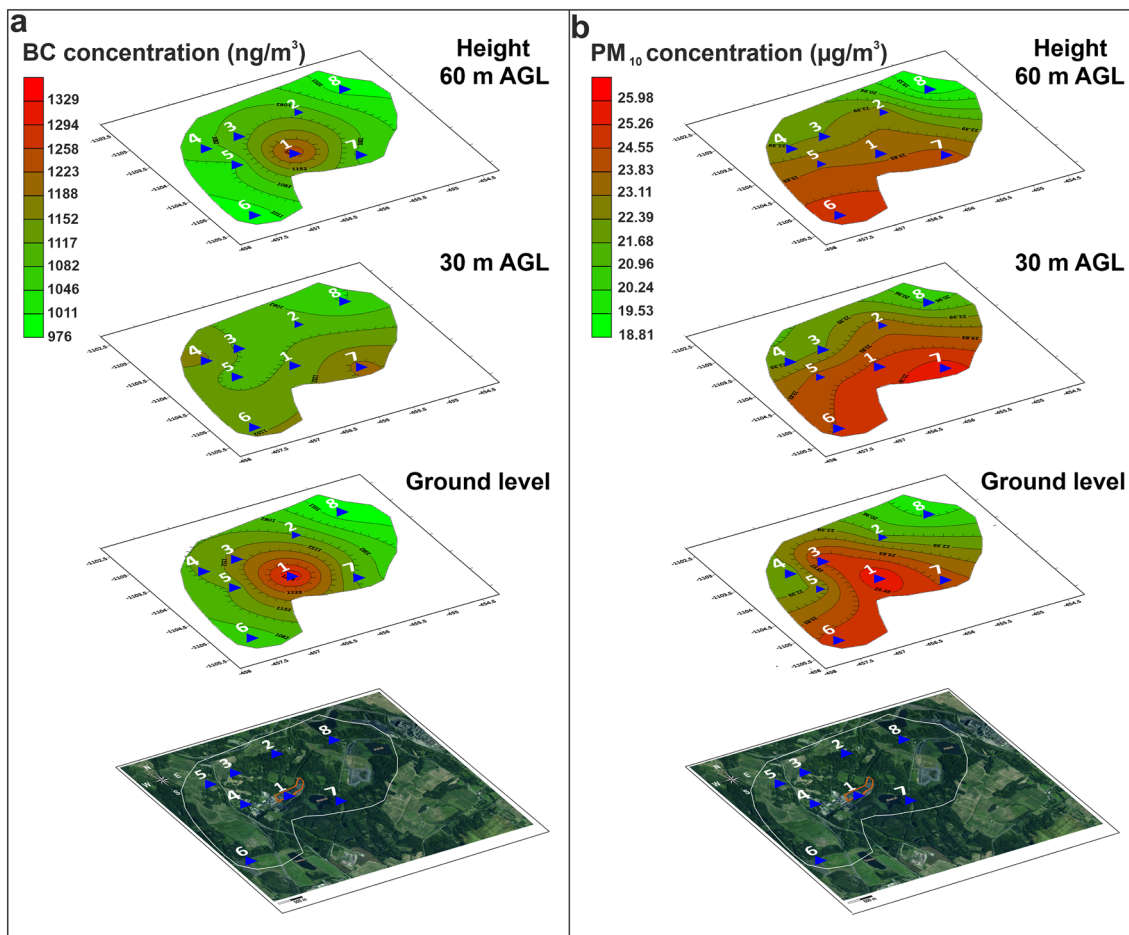
Fig. 6 The distribution of BC (**a**) and PM_{10} (**b**) for ground level, 30 m AGL, and 60 m above ground level

PM_{10} particles have a higher area range and spread over a distance of more than 1 km from the source of the pollution. The highest concentrations of PM_{10} are located in the southwest and southeast streams and do not originate from the coal yard.

Based on the distribution of the concentration within the vertical distribution of the air pollutants, the area studied can be divided into sites with higher concentrations and without significant contamination. These results were confirmed by the cluster analysis (Fig. 7), which was created from the values of BC, PM_{10}, and PM_{10}-TSP concentrations for all the heights studied. The cluster analysis divided the sites into four clusters (Table 5):

- Cluster I, marked as "Coal yard", showed the highest average values of air pollutants except for PM_{10} at altitudes of 30 m AGL and 60 m AGL.
- Cluster II, named "Area N-NW from the coal yard (sites 2, 3, 4, 5)", includes sites with the second lowest concentrations of air pollutants. The wind most often flowed from NW, SE, and N directions during the measurements.

- Cluster III, named "Area SE-SW from the coal yard (sites 6, 7)", includes the second-highest values of PM_{10}-TSP and the highest values of PM_{10} at altitudes of 30 and 60 m AGL.
- Cluster IV, "Not affected area", represents an area without significant load (site 8) with the lowest values of air pollutants at all observed altitudes.

Other sources of pollution near the coal yard and long-distance transport contribute to the resulting pollution around the coal yard.

The grain size distribution of dust particles in total suspended particles

The average percentage of particles in each grain size class in the $\sum$TSP for each site and height is shown in Fig. 8. The results of the one-way ANOVA did not confirm significant differences in particle grain size distribution between heights. The amounts of particles $PM_{<1}$ and $PM_{1-2.5}$ are slightly lower above the body of the coal heap than at other

Fig. 7 The distribution of localities according to the results of cluster analysis
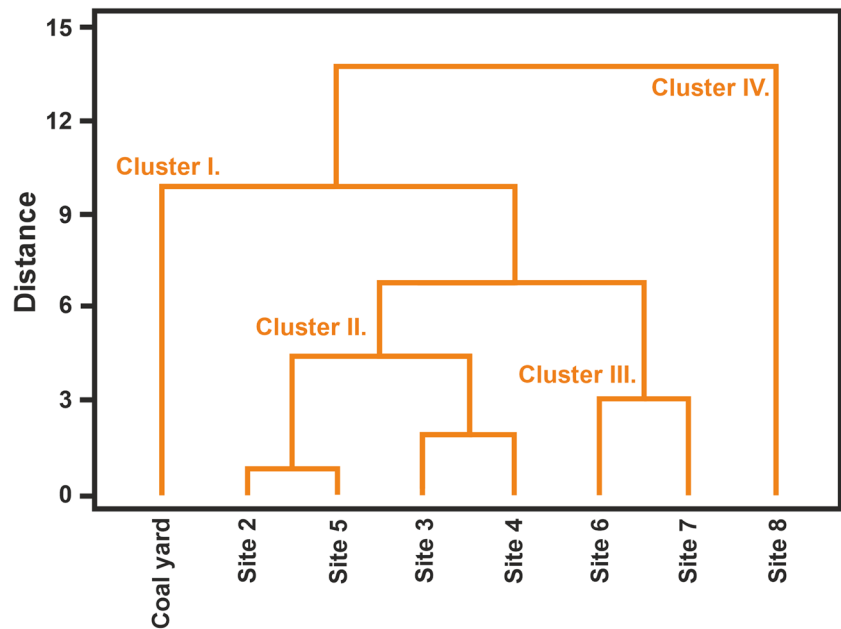
Table 5 Average concentrations of BC, PM_{10}, and PM_{10}-TSP for individual clusters

Cluster	I	II	III	IV
	Coal yard	N-NW from CY	S-SW from CY	Not affected area
BC_GL	1330***	1133	1081**	979*
BC_30 m AGL	1121***	1119.05**	1172	1044*
BC_60 m AGL	1255***	1079	1034**	992*
PM_{10}_GL	25.99***	22.75**	24.52	19.88*
PM_{10}_30 m AGL	24.68	22.99**	25.05***	20.59*
PM_{10}_60 m AGL	23.49	22.87**	24.51***	18.81*
PM_{10}-TSP_GL	20.73***	15.83**	17.24	12.37*
PM_{10}-TSP_30 m AGL	18.58***	14.19**	16.02	12.77*
PM_{10}-TSP_60 m AGL	17.81***	15.05**	16.83	11.33*

*Explanations: * – The lowest concentration; ** – The second lowest concentration; *** – The highest concentration*

sites. In the $\sum$TSP, coarse-grained particles (PM_{10}-TSP) predominate at all monitored sites and heights. The highest average proportion of PM_{10}-TSP particles was found for GL, 30 m AGL, and 60 m AGL at the centre of the coal yard (site No. 1-CY).

The influence of meteorological parameters on air pollutant concentrations

The amount of BC in PM_{10} above the coal surface and in the vertical profile is also influenced by meteorological conditions. Weather conditions play a key role in influencing the resuspension of coal particles, their stay or transport in the air, and the amount of precipitation. Higher concentrations of PM_{10} particles are observed at low wind speeds, and conversely, PM_{10} decreases at higher wind speeds (Cichowicz

et al. 2020). This is due to the greater exchange of the air mass in the assessed area and the displacement of pollutants over greater distances. Also, the current wind direction significantly influences the movement of pollutants from both local and remote sources (Cichowicz et al. 2020). Higher concentrations of BC, TSP, and PM_{10} were observed during rainless days (dry days) than after more heavy rains, which is in line with the results (Zhou et al. 2020).

A statistically significant correlation between the concentration of BC and PM_{10} at all altitudes (1 m, 30 m, and 60 m AGL) was demonstrated in the area studied. PM_{10} show a statistically significant correlation with PM_{10}-TSP at all observed altitudes (Table 6). In terms of meteorological parameters, relative humidity has been shown to show a significant correlation with PM_{10} at all observed altitudes. For particles of the grain size class PM_{10}-TSP,

Fig. 8 (**a**) Average percentage of particles in each grain class in $\sum$TSP depending on height for all sites; (**b**) average percentage of BC particles in PM_{10} depending on height for all sites
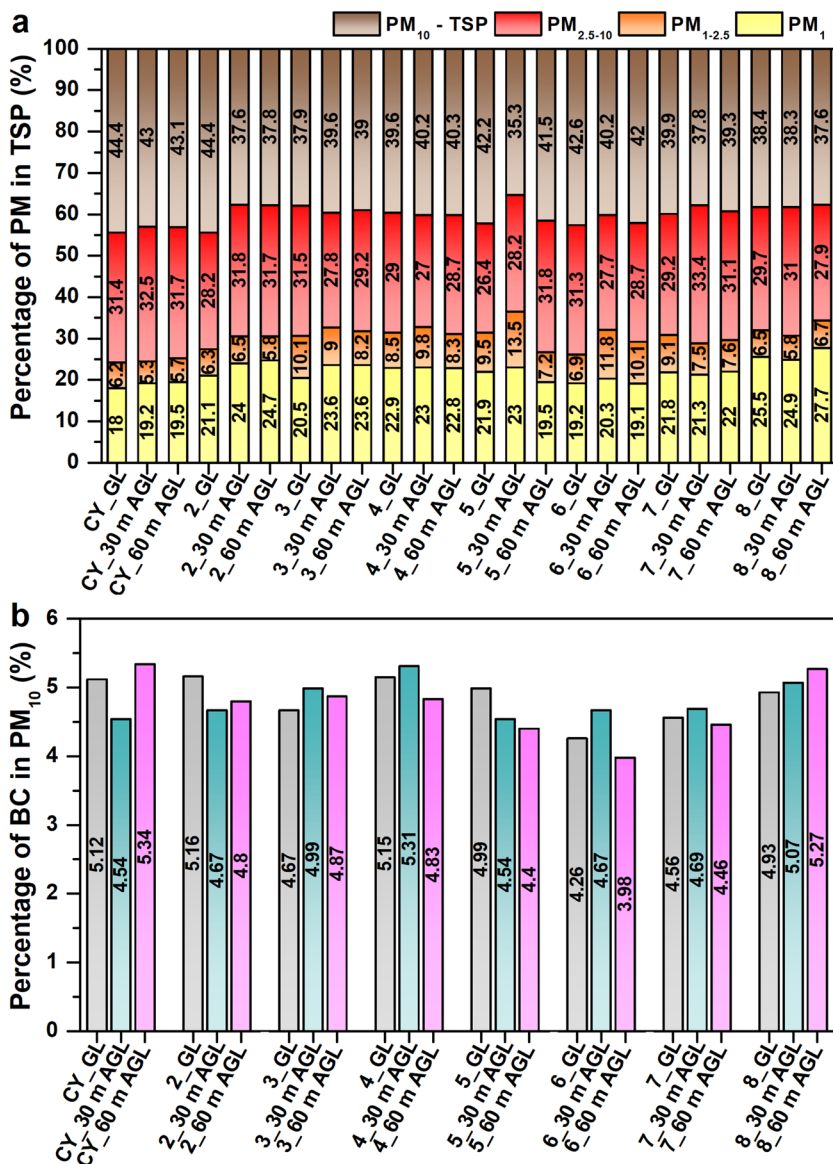

Table 6 The values of the correlation coefficient for monitored parameters depending on height

	GL			30 m			60 m		
	BC	PM_{10}	PM_{10}-TSP	BC	PM_{10}	PM_{10}-TSP	BC	PM_{10}	PM_{10}-TSP
PM_{10}	0.70*			0.67*			0.72*		
PM_{10}-TSP	0.15	0.58*		0.02	0.61*		0.28	0.67*	
Wind speed	-0.44	-0.64*	-0.46	-0.51	-0.57*	-0.47	-0.55	-0.54	-0.31
Wind direction	-0.18	-0.46	-0.69*	-0.01	-0.47	-0.57*	-0.13	-0.33	-0.54*
Relative humidity	0.26	0.63*	0.52	0.25	0.62*	0.72*	0.21	0.53*	0.58*
Temperature	0.36	0.04	-0.61*	0.53	-0.10	-0.63*	0.40	0.01	-0.63*

*Explanation: * Correlation is significant at the 0.05 level*

a significant relative humidity dependence was found only at 30 m AGL and 60 m AGL. Higher concentrations of pollutants were measured at higher relative humidity values. No statistically significant correlation was found

between the concentration of BC and relative humidity. This result is probably related to the hygroscopic nature of BC particles. Fresh, young black carbon particles exhibit hydrophobic properties, but during ageing, they

undergo a hygroscopic transformation, becoming more capable of absorbing water from the surrounding air (Derouin 2021).

Wind speed is another important parameter influencing PM_{10} concentrations. An inverse correlation between wind speed and PM_{10} concentrations was observed at ground level and 30 m AGL. Higher wind speeds were associated with lower PM_{10} concentrations. PM_{10} concentrations at wind speeds ranging from 0.12 to 0.4 m/s were 25.46 ± 7.60 µg/m^3, while at wind speeds ranging from 0.5 to 0.7 m/s, they were lower (15.83 ± 2.10 µg/m^3). Air temperature does not significantly affect BC or PM_{10} concentrations, but it does affect PM_{10}-TSP concentrations at all observed heights. No correlation between air pollution and air pressure values was demonstrated.

Daily variation in BC and PM_{10} concentrations on measurement days

One-way ANOVA was used to monitor the statistical significance of the differences in daily variability. The significance of the differences in the concentration of different particles (BC, $PM_{<1}$, $PM_{1-2.5}$, $PM_{2.5-10}$, PM_{10}-TSP) at heights of 1 m, 30 m, and 60 m AGL for each measurement day was assessed. The analyses did not confirm statistically significant differences in the concentration of particles at heights of 1 m, 30 m, and 60 m AGL on the measurement days.

Within the daily variation in BC and PM_{10} concentrations, average daily concentrations of BC and PM_{10} (Fig. 9) were generated for the studied area (eight sites). The results of the daily variation in air pollutant concentrations showed that average BC and PM_{10} concentrations were mostly highest at ground level and decreased slightly or remained similar with increasing height.

Fig. 9 Average daily concentrations at monitored heights for all locations with the indication of relative humidity (RH) and wind direction (**a**) BC; (**b**) PM_{10}
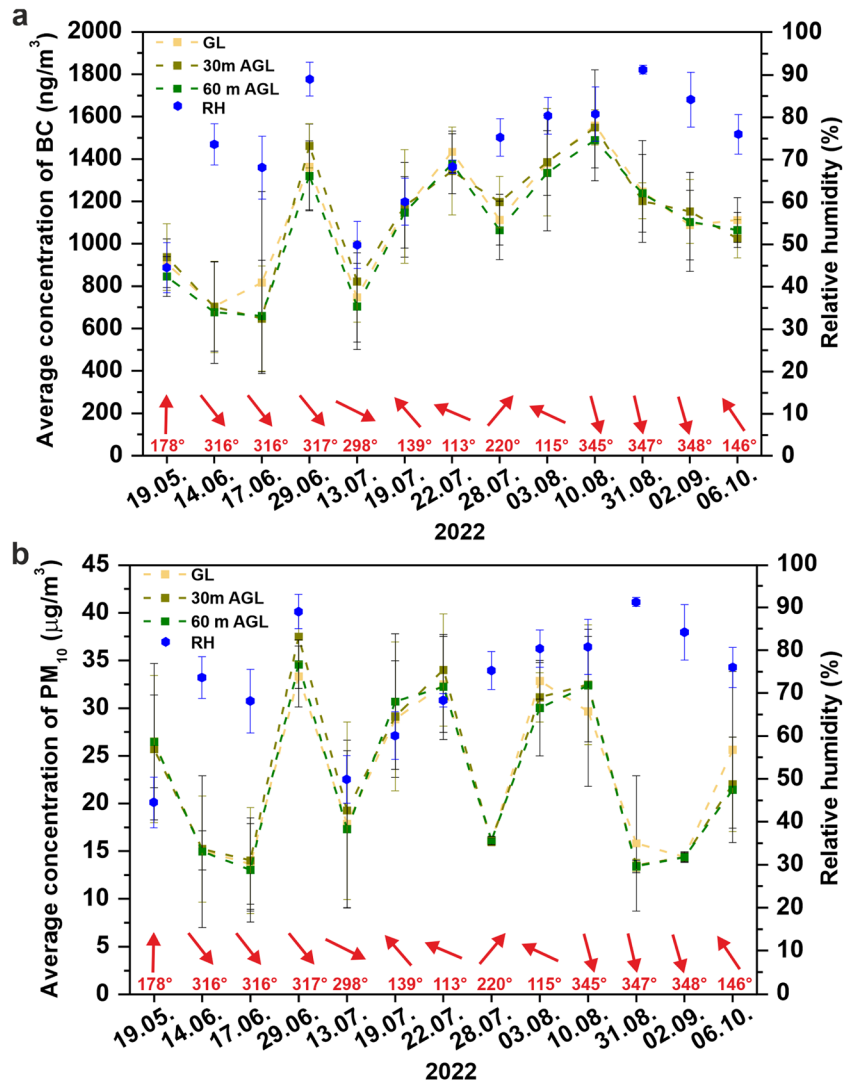
The highest levels of daily BC concentrations were measured on 10 August 2022 at all monitored altitudes. This day resulted in higher concentrations of PM_{10}, especially at altitudes of 30 m AGL and 60 m AGL. Winds from the northern direction probably contributed partially to long-range particle transport, which increased BC and PM_{10} concentrations at these altitudes compared to ground level. The $PM_{<1}$ ratio in $\sum$TSP was 18.21% for 30 m AGL and 17.14% for 60 m AGL. A weekly rain-free period and a temperature higher than 30 °C contributed to the accumulation of BC in the air.

The lowest average values of BC concentration at all altitudes were found on 14 June 2022 and 17 June 2022. On 17 June 2022, the lowest average values of PM_{10} at ground level and at 60 m AGL were also found. On 17 June 2022, coarse-grained particles from the grain size class 10–100 μm (PM_{10}-TSP) predominated in the total amount of TSP, accounting for about 50% of the particles at all observed altitudes. On this day, local sources of emissions had a significant impact on air quality.

On 29 June 2022, the highest PM_{10} concentration values were reached at all monitored altitudes. Approximately one-third of all particles in the $\sum$TSP were less than 1 μm, and one-third had a size of 10–100 μm. In this case, the particles came from both local sources and long-range transport. On 29 June 2022, the study area recorded one of the lowest average wind speed values (0.15 ± 0.13 m/s) and the second highest relative humidity value (89.00 ± 3.96%). Fine-grained PM_1 and $PM_{2.5}$ particles are produced by secondary processes during oxidation, ageing or photochemical reactions of primary emissions during the long-range transport of primary pollutants (Kwon et al. 2023). Particularly, PM_1 particles come from long-range transport (Hien et al. 2021). Based on the results (Hien et al. 2021; Kwon et al. 2023), it can be assumed that the $\sum$TSP on 31 August 2022 was affected by the long-range transport of particles. The $\sum$TSP was predominantly formed by fine-grained PM < 1 μm, representing 67.5% at GL level, 90.8% at 30 m AGL, and 92.1% at 60 m AGL.

Daily variability in BC and PM_{10} concentrations does not affect height, but differences occur between measurement days. The situation in the focus area is influenced by both local emission sources and long-range particle transport. Long-range transport accounted for a particularly significant share of the total TSP ($\sum$TSP) content on 28 July 2022, 31 August 2022, and 2 September 2022, with $PM_{<1}$ accounting for the majority of the total TSP content at all monitored heights (from 66.7% to 95.1%). The size distribution of the particles showed that about 1/3 of the period was affected by particles originating from long-distance transport. These results are important for understanding the sources of pollution and can lead to effective measures to protect the environment and the health of the population. The analysis of the backward tr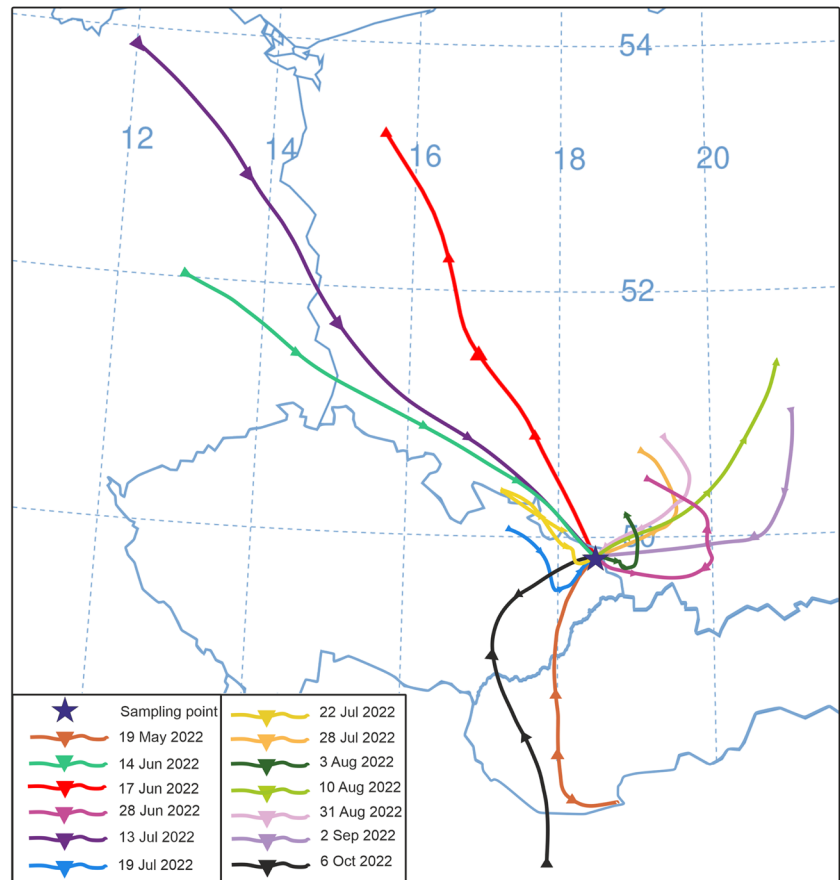ajectories performed by HYSPLIT confirmed that the emission load on 29 June 2022, 28 July 2022, 31 August 2022, and 2 September 2022, was influenced by the long-distance transport from the border area of Poland. Almost similar backward trajectories and wind directions were observed on these days (see Fig. 10). On these days, the air masses flowed from relatively short distances from the border area of the Silesian Voivodeship and the peripheral western part of the Lesser Poland Voivodeship in Poland. Silesia, the second most populous and most urbanised region in Poland, is characterised by coal mining and the associated industry, as well as electricity and heat generation. The Upper Silesia region is still the largest coal basin in Europe (Wehner et al. 2017). With the NW and N flow (from the border area of Poland), there is a significant increase in PM_1 concentrations in the TSP for the study area.

Conclusion

The use of unmanned aerial vehicles represents an important route for obtaining more accurate information on air pollution and the behaviour of some pollutants that can spread from coal yards. Coal particles are released into the environment during coal handling at the coal yard and as a result of weather conditions. The surface-level distribution model for coal particles shows that the anomaly caused by the operation of the coal yard has a very limited extent. The extent of coal particle pollution from the coal yard ranges from a maximum of 500 to 1,000 m. The spatial distribution was monitored for BC particles at ground level (1 m AGL), 30 m AGL, and 60 m AGL. The average BC concentration decreases with the height above the coal surface. The highest average BC concentration at the centre of the coal yard was measured for the ground level at $1,330 \pm 322.8$ ng/m³. Based on the results found and compared with the difference between the background values, BC particles at the centre of the coal yard were found to be made up of 17% coal particles associated with the activities carried out at the coal yard. The average percentage of coal particles in PM_{10} was almost comparable for measurements at different heights and locations, clearly demonstrating that the coal yard does not affect the air pollution load in the surrounding area. The low elevation dispersion of coal particles confirms the limited pollution range area. Modern approaches using UAV techniques allow for more accurate results and better detection of fugitive emissions within the vertical distribution of coal and dust particles from coal yards. Information on the area and spatial distribution of black carbon in PM_{10} can be used to set concentration limits that will be safe regarding the maximum environmental load.

Fig. 10 HYSPLIT backward trajectories for individual measurement days in 2022

Declarations

References

AethLabs (2018) MicroAeth® MA Series MA200, MA300, MA350 operating manual

Arregocés HA, Rojano R, Restrepo G (2022) Meteorological factors contributing to organic and elemental carbon concentrations in PM_{10} near an open-pit coal mine. Environ Sci Pollut Res 29:28854–28865. https://doi.org/10.1007/s11356-022-18505-7

Blackwood TR, Wachter RA (1978) Source assessment: coal storage pile. U.S. Environmental Protection Agency, Washington, DC, USA

Burgués J, Marco S (2020) Environmental chemical sensing using small drones: A review. Sci Total Environ 748:141172. https://doi.org/10.1016/j.scitotenv.2020.141172

Cavalli F, Alastuey A, Areskoug H et al (2016) A European aerosol phenomenology -4: Harmonized concentrations of carbonaceous aerosol at 10 regional background sites across Europe. Atmos Environ 144:133–145. https://doi.org/10.1016/j.atmosenv.2016.07.050

Cheng J, Zheng X, Lei Y et al (2021) A compound binder of coal dust wetting and suppression for coal pile. Process Saf Environ Prot 147:92–102. https://doi.org/10.1016/j.psep.2020.08.031

Chiliński MT, Markowicz KM, Kubicki M (2018) UAS as a Support for Atmospheric aerosols research: case study. Pure Appl Geophys 175:3325–3342. https://doi.org/10.1007/s00024-018-1767-3

Chilinski MT, Markowicz KM, Markowicz J (2016) Observation of vertical variability of black carbon concentration in lower troposphere on campaigns in Poland. Atmos Environ 137:155–170. https://doi.org/10.1016/j.atmosenv.2016.04.020

Cichowicz R, Wielgosiński G, Fetter W (2020) Effect of wind speed on the level of particulate matter PM_{10} concentration in atmospheric air during winter season in vicinity of large combustion plant. J Atmospheric Chem 77:35–48. https://doi.org/10.1007/s10874-020-09401-w

Czech Hydrometeorological Institute (2023a) Information about the establishment: Veolia Energie Czech Republic, a.s. - Heating plant ČSA. In: EMIS. https://www.chmi.cz/files/portal/docs/uoco/web_generator/plants/CZ080/664100371_CZ.html. Accessed 18 Apr 2023

Czech Hydrometeorological Institute (2023b) Information about the establishment: Veolia Energie Czech Republic, a.s. - Heating plant Karviná. In: EMIS. https://www.chmi.cz/files/portal/docs/uoco/web_generator/plants/CZ080/664100101_CZ.html. Accessed 18 Apr 2023

Davis EC, Boegly, WJ Jr (1978) A review of the literature on leachates from coal storage piles. Springfield, VA, USA

Deng X, Li F, Li Y et al (2015) Vertical distribution characteristics of PM in the surface layer of Guangzhou. Particuology 20:3–9. https://doi.org/10.1016/j.partic.2014.02.009

Derouin S (2021) How long do black carbon particles linger in the atmosphere? Eos 102:. https://doi.org/10.1029/2021EO163052

Duan Z, Jiao Q, Wang Y, et al (2023) Effects of hole shape and bottom gap on the flow characteristics behind butterfly porous fence and its application in dust diffusion control in large open-air piles. Environ Sci Pollut Res https://doi.org/10.1007/s11356-023-26293-x

Dubey R, Patra AK, Joshi J et al (2022a) Evaluation of vertical and horizontal distribution of particulate matter near an urban roadway using an unmanned aerial vehicle. Sci Total Environ 836:155600. https://doi.org/10.1016/j.scitotenv.2022.155600

Dubey R, Patra AK, Nazneen (2022b) Vertical profile of particulate matter: A review of techniques and methods. Air Qual Atmosphere Health 15:979–1010 https://doi.org/10.1007/s11869-022-01192-1

Commission E (2019a) Commission Delegated Regulation (EU) 2019/945 of 12 March 2019 on unmanned aircraft systems and on third-country operators of unmanned aircraft systems. Off J Eur Union 152:1–40

Commission E (2019b) Commission Implementing Regulation (EU) 2019/947 of 24 May 2019 on the rules and procedures for the operation of unmanned aircraft (Text with EEA relevance.). Off J Eur Union 152:45–71

Falabella AD, Wallin DO, Lund JA (2018) Application of a customizable sensor platform to detection of atmospheric gases by UAS. In: 2018 International Conference on Unmanned Aircraft Systems (ICUAS). IEEE, Dallas, TX, pp 883–890

Giordan D, Adams MS, Aicardi I et al (2020) The use of unmanned aerial vehicles (UAVs) for engineering geology applications. Bull Eng Geol Environ 79:3437–3481. https://doi.org/10.1007/s10064-020-01766-2

Hakala S, Vakkari V, Bianchi F et al (2022) Observed coupling between air mass history, secondary growth of nucleation mode particles and aerosol pollution levels in Beijing. Environ Sci Atmospheres 2:146–164. https://doi.org/10.1039/D1EA00089F

Hansen ADQ (2005) The Aethalometer

Hedworth H, Page J, Sohl J, Saad T (2022) Investigating errors observed during UAV-based vertical measurements using computational fluid dynamics. Drones 6:253. https://doi.org/10.3390/drones6090253

Hien PD, Bac VT, Thinh NTH, et al (2021) A comparison study of chemical compositions and sources of PM1.0 and $PM_{2.5}$ in Hanoi. Aerosol Air Qual Res 21:210056. https://doi.org/10.4209/aaqr.210056

Jha A, Muller N (2017) Handle with care: The local air pollution costs of coal storage. National Bureau of Economic Research, Cambridge

Jin H, Zhang Y, Li N et al (2022) Preparation and performance characterization of a new dust suppressant with a cross-linked network structure for use in open-pit coal mines. Environ Sci Pollut Res 29:7001–7013. https://doi.org/10.1007/s11356-021-15329-9

Jin L, He Q, Jiang H et al (2020) Unmanned aerial vehicle observations of the vertical distribution of particulate matter in the surface layer of the Taklimakan Desert in China. Atmosphere 11:980. https://doi.org/10.3390/atmos11090980

Kim S, Kim J, Choi I et al (2020) Estimating fugitive particle emission from coal storage yard of thermal power plant using the flux-gradient method. Atmos Environ 243:117860. https://doi.org/10.1016/j.atmosenv.2020.117860

Kurniawan S, Huboyo HS, Samadikun BP (2021) Prediction of coal dust dispersion to total suspended particulate (TSP) concentration in ambient air quality, case study: PLTU Tanjung Jati B. IOP Conf Ser Earth Environ Sci 623:012035. https://doi.org/10.1088/1755-1315/623/1/012035

Kwon S, Won SR, Lim HB, et al (2023) Relationship between $PM_{1.0}$ and $PM_{2.5}$ in urban and background areas of Republic of Korea. Atmospheric Pollut Res 101858. https://doi.org/10.1016/j.apr.2023.101858

Larson A (2015) Fugitive dust mitigation solutions for coal stockpiles. Power

Lee S, Hwang H, Lee JY (2022) Vertical measurements of roadside air pollutants using a drone. Atmospheric Pollut Res 13:101609. https://doi.org/10.1016/j.apr.2022.101609

Liu B, Wu C, Ma N et al (2020) Vertical profiling of fine particulate matter and black carbon by using unmanned aerial vehicle in Macau. China Sci Total Environ 709:136109. https://doi.org/10.1016/j.scitotenv.2019.136109

Liu X, Hadiatullah H, Zhang X et al (2021a) Analysis of mobile monitoring data from the microAeth® MA200 for measuring changes

in black carbon on the roadside in Augsburg. Atmospheric Meas Tech 14:5139–5151. https://doi.org/10.5194/amt-14-5139-2021

Liu X, Shi X-Q, He H-D et al (2021b) Vertical distribution characteristics of particulate matter beside an elevated expressway by unmanned aerial vehicle measurements. Build Environ 206:108330. https://doi.org/10.1016/j.buildenv.2021.108330

Mueller SF, Mallard JW, Mao Q, Shaw SL (2015a) Variability of natural dust erosion from a coal pile. J Appl Meteorol Climatol 54:3–14. https://doi.org/10.1175/JAMC-D-14-0126.1

Mueller SF, Mallard JW, Mao Q, Shaw SL (2015b) Emission factors for fugitive dust from bulldozers working on a coal pile. J Air Waste Manag Assoc 65:27–40. https://doi.org/10.1080/10962247.2014.960953

Nducol N, Siaka YFT, Yakum-Ntaw SY et al (2021) Preliminary study of black carbon content in airborne particulate matters from an open site in the city of Yaoundé. Cameroon Environ Monit Assess 193:135. https://doi.org/10.1007/s10661-021-08924-3

Ostro B, Spada N, Kuiper H (2023) The impact of coal trains on $PM_{2.5}$ in the San Francisco Bay area. Air Qual Atmosphere Health. https://doi.org/10.1007/s11869-023-01333-0

Palas (2023) Fidas® Frog

Poormorteza S, Gholami H, Rashki A, Moradi N (2022) High-resolution, spatially resolved quantification of wind erosion rates based on UAV images (case study: Sistan region, southeastern Iran). Environ Sci Pollut Res 30:21694–21707. https://doi.org/10.1007/s11356-022-23611-7

Rojano R, Arregocés H, Angulo L, Restrepo G (2016) PM_{10} emissions due to storage in coal piles in a mining industrial area. In: Proceedings of the 24 International Conference th on Modelling, Monitoring and Management of Air Pollution. WIT Transactions on Ecology and The Environment, Crete, Greece, pp 87–97

Rolph G, Stein A, Stunder B (2017) Real-time environmental applications and display system: READY. Environ Model Softw 95:210–228. https://doi.org/10.1016/j.envsoft.2017.06.025

Rovira J, Paredes-Ahumada JA, Barceló-Ordinas JM et al (2022) Nonlinear models for black carbon exposure modelling using air pollution datasets. Environ Res 212:113269. https://doi.org/10.1016/j.envres.2022.113269

Samad A, Alvarez Florez D, Chourdakis I, Vogt U (2022) Concept of Using an Unmanned Aerial Vehicle (UAV) for 3D Investigation of Air Quality in the atmosphere - example of measurements near a roadside. Atmosphere 13:663. https://doi.org/10.3390/atmos13050663

Sekuła P, Bokwa A, Bartyzel J et al (2021) Measurement report: Effect of wind shear on PM_{10} concentration vertical structure in the urban boundary layer in a complex terrain. Atmospheric Chem Phys 21:12113–12139. https://doi.org/10.5194/acp-21-12113-2021

Stein AF, Draxler RR, Rolph GD et al (2015) NOAA's HYSPLIT atmospheric transport and dispersion modeling system. Bull Am Meteorol Soc 96:2059–2077. https://doi.org/10.1175/BAMS-D-14-00110.1

Štrbová K, Raclavská H, Bílek J (2017) Impact of fugitive sources and meteorological parameters on vertical distribution of particulate matter over the industrial agglomeration. J Environ Manage 203:1190–1198. https://doi.org/10.1016/j.jenvman.2017.06.001

Techarat P, Tontiwachwuthikul P (2020) Coal dust dispersion from a coal storage pile. Songklanakarin J Sci Technol 42:557563. https://doi.org/10.14456/SJST-PSU.2020.70

Wang Y, Zhou G, Xu C et al (2020) Synthesis and characteristics of a novel dust suppressant with good weatherability for controlling dust in open coal yards. Environ Sci Pollut Res 27:19327–19339. https://doi.org/10.1007/s11356-020-08309-y

Wehner T, Bierwirth A, Buschka M, et al (2017) Phasing-out coal, reinventing European Regions. Wuppertal Institute for Climate, Environment and Energy, Wuppertal and Berlin.

WHO (2021) WHO global air quality guidelines. World Health Organisation, Geneva

Wittenburg J (2018) Analysis of ambient particulate concentration near a coal storage pile. Dissertation, University of Northern Iowa

Woo J, Shin J, Yoo S-H, Huh S-Y (2023) Reducing Environmental impact of coal-fired power plants by building an indoor coal storage: An economic analysis. Energies 16:511. https://doi.org/10.3390/en16010511

Wyche KP, Cordell RL, Smith ML et al (2020) The spatio-temporal evolution of black carbon in the North-West European 'air pollution hotspot.' Atmos Environ 243:117874. https://doi.org/10.1016/j.atmosenv.2020.117874

Zhou Y, Yue Y, Bai Y, Zhang L (2020) Effects of Rainfall on $PM_{2.5}$ and PM_{10} in the Middle Reaches of the Yangtze River. Adv Meteorol 2020:1–10. https://doi.org/10.1155/2020/2398146

Publisher's Note Springer Nature remains neutral with regard to jurisdictional claims in published maps and institutional affiliations.